Mucin-targeting-aptamer functionalized liposomes for delivery of cyclosporin A for dry eye diseases

Ka-Ying Wong[1,2,] Yibo Liu[1,2], Liping Zhou[1,3,4,5], Man-Sau Wong[1,3,4], Juewen Liu*[1,2]

[1]Centre for Eye and Vision Research (CEVR), 17W Hong Kong Science Park, Hong Kong;
[2]Department of Chemistry, Waterloo Institute for Nanotechnology, University of Waterloo, Waterloo, ON, N2L 3G1, Canada

[3]Department of Food Science and Nutrition, The Hong Kong Polytechnic University, Hung Hom, Kowloon, Hong Kong SAR, PR China

[4]Research Center for Chinese Medicine Innovation, The Hong Kong Polytechnic University, Hung Hom, Kowloon, Hong Kong SAR, PR China

[5] School of Optometry, The Hong Kong Polytechnic University, Hung Hom, Kowloon, Hong Kong SAR, PR China

Authors' email addresses:
Ka-Ying Wong: **kaya.wong@cevr.hk**
Yibo Liu: **xiaonao0526@hotmail.com**
Liping Zhou: **lp.zhou@polyu.edu.hk**
Man-Sau Wong: **man-sau.wong@polyu.edu.hk**
Juewen Liu: liujw@ uwaterloo.ca

Corresponding author: Prof. Juewen Liu (liujw@ uwaterloo.ca)

Author contributions: Ka-Ying Wong conducted the experiments, analyzed the data, and prepared the manuscript. Yibo Liu contributed to designing the experiments and providing advice. Liping Zhou contributed to conducting *in vivo* study. Man-Sau Wong contributed to conceptualizing the topics and providing advice. Juewen Liu contributed to conceptualizing the topic, providing advice, and revising the manuscript.

Disclosure: The authors have filed for patent applications related to this work.

Abstract:

Traditional eye drops are convenient to use; however, their effectiveness is limited by their poor retention time and bioavailability in the eyes due to ocular barriers. Therefore, strategies to enhance ocular drug delivery are required. Herein, we constructed a mucin-1 aptamer-functionalized liposome and loaded it with cyclosporin A, a common ocular drug in eye drops used to treat dry eye diseases (DED). Drug encapsulation reduced the liposome size without changing the surface potential of liposomes. Approximately 90% of the cholesterol-modified aptamers were inserted to the liposomes. We evaluated the cytotoxicity, anti-inflammatory effects, cell permeability regulation, and retention time of liposomes in human corneal epithelial cells under dry eye conditions. These results suggest that the aptamer-functionalized liposomes are more efficient as nanocarriers than non-functionalized liposomes and drug-free liposomes. They restore inflammation levels by 1-fold and remain in the cells for up to 24 h. An *in vivo* study was also performed in a rat DED model, which demonstrated the efficacy of aptamer-functionalized liposomes in restoring tear production and corneal integrity. The present study demonstrated the capability of aptamer-functionalized liposomes in the delivery of ocular drugs for the management of ocular diseases.

Keywords: Cyclosporin A, Aptamer-functionalized liposome, Dry eye diseases, Drug delivery, Mucin-1

Abbreviations:

Cyclosporine A, CsA; Dry eye diseases, Human corneal epithelial cell, HCEC; Interleukin-1β, IL-1β; Interleukin-6, IL-6; Interleukin-8, IL-8; DED; 1,2-Dioleoyl-sn-glycero-3-phosphocholine, DOPC; 1,2-dioleoyl-sn-glycero-3 phosphoethanolamine-N-(lissamine rhodamine B sulfonyl, Rhod PE

1. Introduction

Ocular drug delivery has been a challenging topic as human eyes have static (corneal epithelium, corneal stroma, corneal endothelium, blood-aqueous barrier) and dynamic (tear dilution, conjunctival barrier, and retinal-blood barrier) barriers to prevent external substances, including therapeutic molecules, from getting into the eyes.[1] In the past two decades, the rapid development of ocular drug delivery has provoked newer therapeutic interventions, like liposomes, micelles, polymer nanoparticles, drug-eluting contact lenses, lipid-modified nucleic acids, and ocular inserts, to overcome the ocular barriers, improve drug absorption, drug concentration at the target site, drug retention time and biocompatibility.[1-4] Ocular drug delivery research has also gained significant attention to surface modification of nanoparticles and polymers to achieve sustained and stimuli-responsive drug release.[5, 6]

The functionalization of liposomes with aptamers has broadened the use of liposomes in targeted drug delivery.[7] Aptamers are short single-stranded oligonucleotides that specifically bind to their targets. Aptamers have been demonstrated to have less toxicity or immunogenicity compared to other targeting ligands, like antibodies.[7, 8] Pegaptanib, an RNA aptamer targeting vascular endothelial growth factor, is an FDA-approved drug for age-related macular degeneration.[9] With merits of aptamers in easy synthesis, chemical modification, and lipid conjugation, aptamer-functionalized liposomes have promising targeted-drug delivery in cancer therapy.[10] In this work, we aim to test its application in ocular delivery.

Cyclosporine A (CsA), a hydrophobic endecapeptide molecule, is an FDA-approved ocular drug for dry eye disease (DED).[11] CsA functions as an immunosuppressive agent to reduce inflammation and interfere with tear production.[12] However, CsA possesses low solubility in aqueous solutions, which makes it difficult to deliver it safely and effectively into the eyes.[12-14] Current oil-based CsA eye drops have low bioavailability and require multiple administrations. An aqueous nanomicellar CsA solution has been developed to improve the delivery of CsA into the eye. However, the major route of aqueous CsA absorption in the eyes is through the conjunctiva and sclera and is mainly delivered to the posterior tissues.[13] Also, the target site of DED does not include the posterior segment of the eye.[15] While liposomes have been a popular vehicle for treatment of ocular diseases including DED, most do not have a specific targeting mechanism.[16-24] While cationic materials may increase the retention time, they may also exert toxicity.[25] Therefore, better formulations that can increase the retention time are needed.[24, 25]

Mucin 1 is a glycoprotein that is highly expressed in the corneal epithelium and is located on the cornea as part of the static barrier in the eye. To achieve targeted delivery of CsA to the

cornea, the disease site of DED, the present study aimed to synthesize a site-specific CsA delivery tool using mucin-1 aptamer-functionalized liposomes. Such aptamer-functionalized liposomes have highly tunable formulations in both DNA sequence and lipid composition.[26-31] It is hoped that mucin-1 aptamer-functionalized liposomes could increase the retention time of CsA in the cornea and increase the bioavailability of CsA to improve DED treatment.

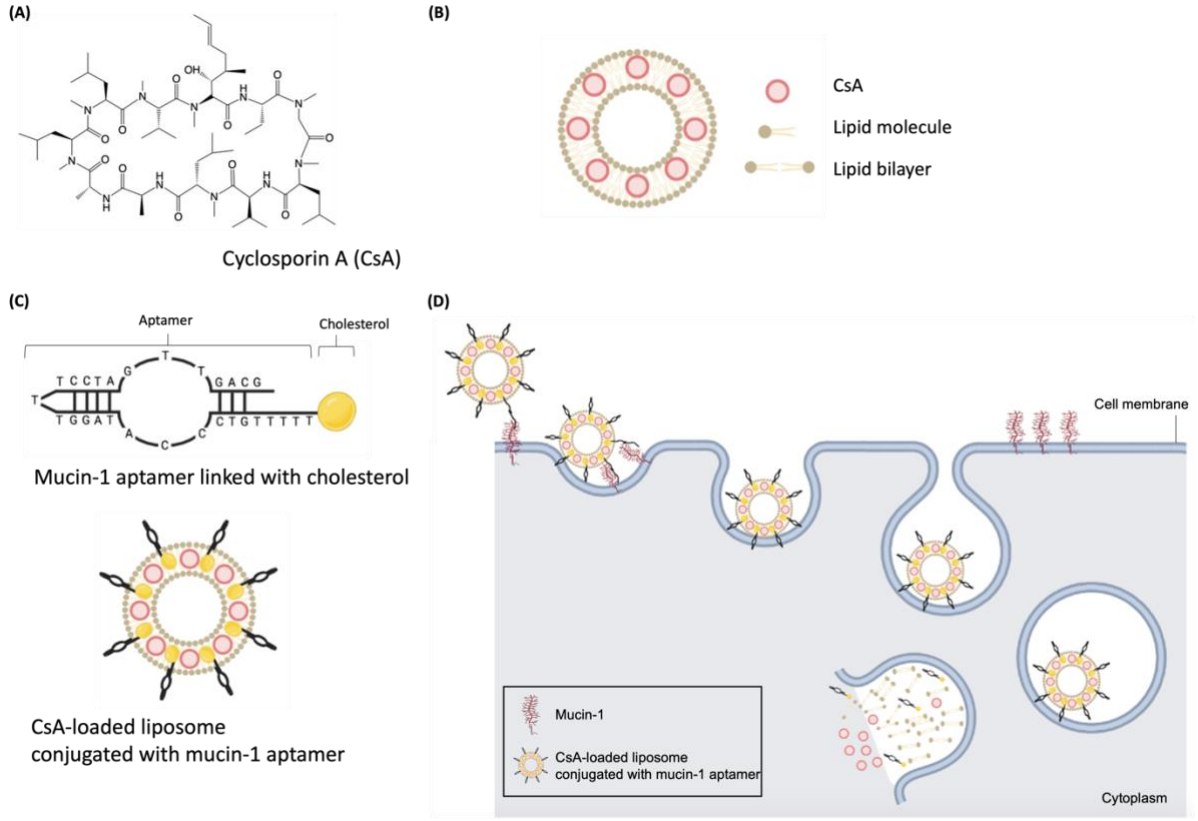

Scheme 1. (A) The structure of CsA. (B) Loading of CsA in the hydrophobic lipid bilayer region of liposomes. (C) The sequence of the mucin-1 binding aptamer with a cholesterol label at the 3′-end, and CsA-loaded liposomes coated with cholesterol-modified mucin-1 aptamer. (D) Delivery of CsA by the liposomes, and the release process in cells.

2. Methodology

2.1 Materials

Phospholipids were purchased from Avanti Polar Lipids. All aptamers and primers were purchased from Integrated DNA Technologies. Cyclosporine, MTT, lissamine green B and Fluoromount™ Aqueous Mounting Medium were purchased from Sigma-Aldrich. Amicon Ultra-0.5 mL Centrifugal Filters were purchased from Millipore Sigma. All the cell culture-related chemicals including medium, serum, and antibiotics were purchased from Fisher Scientific Inc. Culture flasks and Hoechst 33342 solution were purchased from Thermo Fisher. Sodium chloride, Isol-RNA Lysis Reagent were purchased from VWR. PBS, iScript™ cDNA

Synthesis Kit, and SsoFast EvaGreen supermixes were purchased from Bio-Rad. Coverslips were purchased from SPL Life Sciences. Milli-Q water was used to prepare all buffers, solutions, and suspensions. Standardized phenol red-impregnated cotton threads were purchased from FCI Ophthalmics.

2.2 Preparation of CsA liposome

Liposomes were prepared using the standard extrusion method. DOPC (1,2-dioleoyl-sn-glycero-3-phosphocholine) and Rhod PE (1,2-dioleoyl-*sn*-glycero-3-phosphoethanolamine-*N*-(lissamine rhodamine B sulfonyl)) (ammonium salt) at a weight ratio of 99:1 were dissolved in chloroform with a total lipid mass of 2.5mg. CsA in chloroform were mixed into the lipid mixture at various weight percentages (0, 2, 5, 10, 20, 40, 50, 100 wt.% of lipid). The chloroform was removed by blowing with N_2 followed by drying in a vacuum oven overnight at RT. The lipid thin films were then rehydrated and dissolved in 0.5 mL PBS at RT with sonication. The lipid concentration after rehydration was 5 mg/ml. The lipid suspensions were subjected to extrusion with two stacked polycarbonate membranes (100 nm pore size) and two syringes for 11 times at RT. Liposome suspensions were stored at 4 °C until further use.

2.3 Dynamic light scattering (DLS)

20 μL of the freshly extruded liposome samples were diluted 50 times with PBS. The hydrodynamic diameter, polydispersity index (PDI) and zeta potential of the liposomes were determined using dynamic light scattering (Zetasizer Nano, Malvern).

2.4 CsA quantification by UV-vis spectrophotometer

The measurement of CsA in liposomes was performed by UV-vis spectroscopy (Dell OptiPlex GX1) at a fixed wavelength of 205nm. Serial concentrations of CsA dissolved in buffer A (PBS: Ethanol at the ratio of 1:10) were used to construct a standard curve for CsA quantification. To measure total CsA in the liposome suspension, liposomes were obtained by pooling samples from three batches of liposome synthesis. Subsequently, the combined samples were suspended in ethanol at a 1:10 ratio (sample: ethanol) and vortexed for 1 min to destroy the liposome structure and release the loaded CsA into the solution. The samples were further diluted 10 times with buffer A before UV-vis analysis. To measure the unloaded CsA in the liposome suspension, unloaded CsA was separated using 3 k Amicon Ultra-0.5 mL Centrifugal Filters (14,000 rpm, 10 min). The filtrates (20 μL) were diluted with ethanol (200 μL) before the UV-vis measurements. The CsA content in the samples was determined by subtracting the absorbance of liposomes alone from that of CsA liposomes and was compared with the standard curve.

2.5 Determination of encapsulation efficiency and drug loading

The encapsulation efficiency and drug-loading content of the CsA in liposomes were calculated according to the following equations:

Drug loading content (%) = (Weight of CsA in Liposome / Weight of liposome) X 100

Encapsulation efficiency (%) = (Weight of total CsA – weight of unloaded CsA)/ Weight of initial CsA) X 100

2.6 Aptamer functionalization and analysis

A 25-base aptamer sequence, S2.2 aptamer, was found to have relatively high affinity and specificity to MUC 1.32 To insert the S2.2 aptamer with unloaded liposomes (aptamer liposomes) or CsA liposomes (aptamer CsA liposomes), Mucin-1 aptamer with cholesterol (Chol) at the 3′-end (S2.2: 5′-GCAGTTGATCCTTTGGATACCCTGGTTTTT-Chol-3′) was used. The liposome suspension (20 µL, 5 mg/mL) was mixed with 10 µL of aptamer (100 µM) in 20 µL PBS, 20 µL NaCl (pH 7.5, 5 M), and MilliQ water to achieve a final volume of 200 µL. After overnight incubation, the free aptamer was separated from the liposome by ultracentrifugation (Beckman Optima TLX Ultracentrifuge) at 120,000 rpm for 30 min. The concentration of the free aptamer was measured using a spectrophotometer (Tecan Spark) at 260 nm. The liposome pellets were resuspended in 20 µL PBS (liposome concentration, 5 mg/ml). A non-aptamer (B2: 5′-ACTTCAACATCTAGCTGGTGG-Chol-3′) was inserted to CsA liposomes (non-aptamer CsA liposomes) as a negative control.

2.7 Human corneal epithelial cell (HCEC) culture and hyperosmotic stress induction

HPV-immortalized HCECs were gifted from Dr. Maud Gorbet at the University of Waterloo. The culture method was based on Dr. Gorbet's method with a few modifications.[32] The cells (passage 4-9) were maintained in DMEM/F12 medium supplemented with 1% FBS and 1% penicillin/streptomycin at 37 ºC, 95% humidity and 5% CO2. The cell medium was changed every 2 days. To establish an *in vitro* DED model, sodium chloride was added to the culture medium to increase the osmolarity of the medium by 200 mOsM from 312 mOsM to 512 mOsM. 5 M sodium chloride stock in MilliQ water (10,000 mOsM) was prepared. To increase the osmolarity of the medium by 200 mOsM, 1 mL 5 M sodium chloride was added to 49 mL medium.

2.8 Cell viability

HCECs were seeded in 96-well plates at a density of 12,000 cells/well and were incubated for 24 h. Afterward, the cells were treated with either vehicle, CsA (0.002%, 0.001%, and 0.0001% in medium), drug-free liposomes, or CsA liposomes (at concentrations of 0.5, 5, and 50 µg/mL

liposomes) in serum-free hyperosmolarity medium for 24 h. HCECs cultured in isosmotic medium with vehicle were used as a control. Next, cells were incubated with 0.5mg/ml MTT for 4 h. The medium was then discarded, and 100 µL of DMSO was added to each well to dissolve the precipitates. Finally, the absorbance was measured at 570 nm using a Microplate Reader (Tecan Spark).

2.9 Cellular uptake

To assess cellular uptake in 4 h, HCECs were seeded onto cell culture-grade coverslips in 48-well plates at a density of 25,000 cells per well for 24 h. Subsequently, the cells were treated with non-aptamer CsA liposomes, aptamer liposomes, or aptamer CsA liposomes (at a concentration of 5 µg/mL liposomes) in serum-free hyperosmolarity medium for 4 h.

To evaluate liposome retention in cells, HCECs were treated with liposomes for 4 h, as described, followed by a 20-h incubation in hyperosmolarity medium after washing with PBS. HCECs cultured in an isosmotic medium were used as a control. After either 4 or 24 h of incubation, cells on coverslips were washed twice with ice-cold PBS and then fixed with fresh 4% paraformaldehyde for 15 min at room temperature. Next, the cells were stained with 1 µg/mL Hoechst 33342 in PBS for nucleus staining for 1 minute at room temperature. The coverslips were mounted on glass microscope slides with a drop of Fluoromount™ Aqueous Mounting Medium to reduce fluorescence photobleaching and sealed with nail polish. Fluorescence images were captured at the mid-plane of cells using a Nikon Eclipse Ti Inverted Research Microscope with a magnification of 400X. The excitation wavelengths of Hoechst and Rh-PE were 361 nm and 560 nm, respectively. The fluorescence intensity was measured by Image J.

2.10 Real-time PCR

HCECs were seeded in 6-well plates at a density of 250,000 cells/well and incubated for 24 h. Afterward, the cells were treated with CsA (0.001% and 0.0001% in medium), non-aptamer CsA liposomes, aptamer liposomes, or aptamer CsA liposomes (0.5 and 5 µg/mL liposomes) in serum-free hyperosmolarity medium for 4 h. After treatment, the cells were washed twice with PBS to remove unbound liposomes and CsA and then incubated for an additional 20 h in hyperosmolarity medium. HCECs cultured in isosmotic medium with vehicle were used as a control. 24 h after cell seeding, RNA was extracted from the cells using Isol-RNA Lysis Reagent, and reverse transcription was performed using the iScript™ cDNA Synthesis Kit according to the manufacturer's instructions. The expression levels of target genes, including interleukin-1β (IL-1β), interleukin-6 (IL-6), interleukin-8 (IL-8), and glyceraldehyde-3-

phosphate dehydrogenase (GAPDH), were measured using SsoFast EvaGreen with specific primer pairs (**Table S1**). The gene expression was normalized to GAPDH.

2.11 Cell membrane permeability

HCECs were seeded on cell culture-grade coverslips in 48-well plates at a density of 25,000 cells/well and incubated for 24 h. The cells were treated as described in Section 2.10. After treatment, the medium was aspirated and the cells were rinsed twice with PBS. The membrane integrity was assessed using rose bengal staining and fluorescein uptake assays. For the rose bengal assay, the cells were incubated with 0.1% rose bengal in PBS for 5 min. The solution was then discarded, and the cells were washed with PBS. The rose bengal uptake by the cells was visualized and captured at a magnification of 600X using a Celestron 44348 Pentaview LCD Digital Microscope. For the fluorescein uptake assay, the cells were incubated with 1 mM fluorescein in the medium for 5 min, after which the solution was discarded, and the cells were washed with PBS. Fluorescein uptake was visualized and captured as described in section 2.9, with an excitation wavelength of 498 nm. The overall intensity of the fluorescent signals was quantified using the corresponding Nikon system.

2.12 Animal study

18 healthy male SD rats aged 8 weeks were purchased from Beijing Vital River Laboratory Animal Technology Co., Ltd., and housed in the animal facilities of Sino Animal under a 12-h light/dark cycle at a temperature of 25 ± 2°C and relative humidity of 40 ± 5%. The experimental protocol was approved by the Animal Ethics and Welfare Committee (Sino Animal, 20220004MSE). The liposomes were prepared in the University of Waterloo and shipped to Beijing for testing. After one week of adaptation, dry eye disease was induced in rats by twice-daily topical installation of 0.2% benzalkonium chloride (BAC) at 5 μL per installation for 7 consecutive days. Following this, the rats were randomly assigned into three groups of 6 rats each and received the following treatments for 28 consecutive days, twice a day (at 10 a.m. and 4 p.m.): 1) 20 μL of PBS as the DED model group, 2) 20 μL of Cycloome® 0.05% CsA eye drops (SINQI, China) as the positive control group, and 3) 20 μL of sterile aptamer CsA liposomes (0.5 mg/mL) as the experimental group. The CsA amount in each installation was 10 μg and 0.89 μg in the positive control group and experimental group, respectively.

2.13 Fluorescein staining for corneal integrity

A total of 5 μL of 0.1% lissamine green B was applied to the lateral conjunctival sac of the rats. After three forced blinks, the fluorescein distribution was observed with low-brightness cobalt blue light under a digital slit lamp (SUN Kingom, LS-6). The fluorescein punctate staining

score was measured following the National Eye Institute-recommended system. The cornea was divided into 5 zones (central, superior, temporal, nasal, and inferior) and for each zone, the severity of corneal fluorescein staining was graded on a scale from 0 to 3. The scores from 5 zone were then added up with a maximum score of 15.[33]

2.14 Tear production

The aqueous tear production was measured with standardized phenol red-impregnated cotton threads (FCI Ophthalmics, Pembrooke, MA) before treatment as a basal level of tear production in DED model and after the last treatment. The threads were put into the lateral canthus for 60 s, and the wetting length of the thread was measured as an indication of tear production.

2.15 Statistical analysis

For MTT, RT-PCR, and cell cellular uptake assays, the data were reported as mean ± SEM. Inter-group differences were analyzed by one-way ANOVA with Tukey's as a post hoc test. A value of $P < 0.05$ was considered statically significant. All graphs in this study were plotted by using GraphPad Prism Version 9.0. Three independent trials were conducted for *in vitro* study.

3. Results and discussion

Synthesis and characterization of aptamer CsA liposomes

The lipid composition of liposomes determines their physiochemical properties, which has already had a major impact on many biomedical areas.[34] Using partial lipid composition of the cell membrane is a widely used strategy for drug delivery.[34, 35] We adopted DOPC in the present study because it is the dominant component of the phospholipid bilayer of cell membranes. In addition, 1% rhodamine-labelled PE (Rhod PE) was used as an indicator to visualize liposomes in cells.

CsA is a hydrophobic molecule which could be trapped in the bilayer region of liposomes (Scheme 1A). To optimize the best loading condition, we co-dissolved the lipids and CsA at 2, 5, 10, 20, 40, 50, and 100, wt.% of lipid in chloroform, which was then subjected to thin-film hydration and extrusion to achieve liposomes close to the size of membrane pore (100 nm). Since CsA is a hydrophobic molecule, it should be in the bilayer region of the liposomes (Scheme 1B). We analyzed the size and zeta potential of liposomes using DLS. **Figure 1A** showed that the unloaded liposomes had a mean particle size of 157 nm. The mean size of liposome decreased with increasing CsA loading from 2 wt.% (156 nm) to 50 wt.% (93 nm). In **Figure S1**, liposomes with CsA loading of 2-20 wt.% had a narrow size distribution profile with lower PDI (<0.15). However, large aggregates and higher PDI (>0.15) were observed in

liposomes loaded with 40, 50, and 100 wt.% CsA, which could be due to instability. The size of liposomes could be affected by the lipid packing and composition in the phospholipid layer of liposomes.[36, 37] Instability can lead to particle agglomeration. In this study, the hydrophobic CsA drug was packed into the phospholipid layer, potentially affecting the liposome size and lipid packing. While increased CsA loading resulted in a smaller liposome size, the addition of high amounts of CsA (starting from 40 wt.%) caused CsA and lipid molecules to agglomerate. Thus, we 20wt.% CsA was the maximal drug loading while still keeping stable liposomes. In addition, no significant changes were observed in the zeta potential of liposomes in all samples (**Figure 1B**).

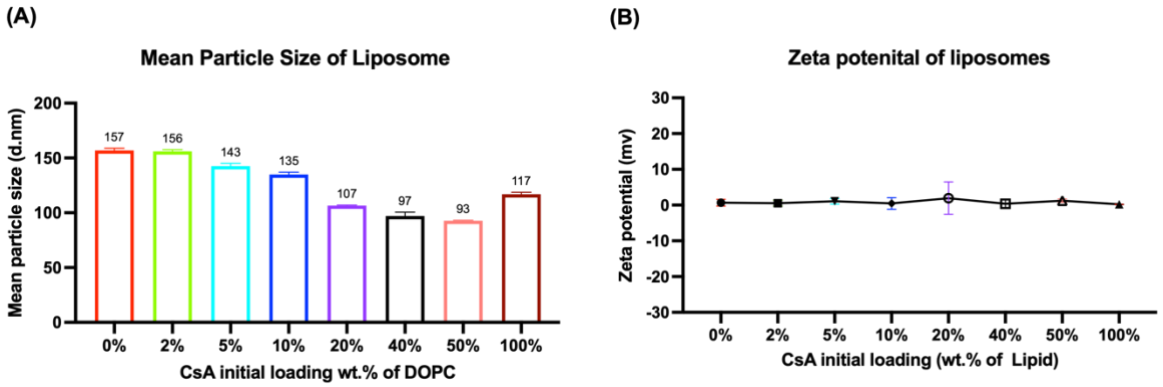

Figure 1 Characterization of the synthesized liposomes. (A) The mean particle size of the synthesized liposomes with different CsA loadings analyzed using DLS. (B) The zeta potential of the liposomes with different CsA loadings analyzed using DLS, n=3.

We used UV-vis spectroscopy to quantify the CsA in samples. CsA had a peak UV absorbance at around 210 nm when dissolved in ethanol.[38] In the present study, we constructed a calibration curve using PBS: ethanol at a 1:10 ratio as the solvent. Based on the UV spectra and calibration curve (**Figure S2**), CsA had a peak absorbance at 205 nm. The R^2 value of the calibration curve was 0.9922. After subtracting the background absorbance in unloaded liposomes and comparing the UV absorbance of the samples to the calibration curve (**Figure S3**), the total CsA and unloaded CsA in the four liposome suspensions were determined (**Table S2**). The total CsA contents in the 10, 20, 40 and 50 wt.% samples were 503, 895, 605 and 772 μg/mL, while the unloaded CsA contents in 10, 20, 40 and 50 wt.% samples were 10.1, 17.1, 23.8 and 29.9 μg/mL, respectively. The purpose of selecting samples with 10, 20, 40, and 50 wt.% was to compare the loading efficiency between samples that have uniform size and those that have aggregation. The drug loading content and encapsulation efficiency were also calculated (**Table S2**). In general, an optimum loading condition could achieve an entrapment efficiency

of around 90% or more.[39] Although 10 wt.% CsA group had over 90% encapsulation efficiency, the 20 wt. % CsA group had the highest CsA content (17.6%) with a comparable encapsulation efficiency (87.8%). Therefore, considering the stability and loading capacity, the 20 wt.% CsA group was subjected to aptamer functionalization and biological studies.

The S2.2 mucin 1 aptamer reported by the Ferreira group was adopted in the present study.[40] It has a reported K_d value of 0.13 μM toward mucin 1. Mucin 1 is a membrane-associated heavy molecular glycoprotein responsible for lubricating the ocular surface to facilitate smooth blinking, forming a smooth spherical surface for vision, providing an ocular barrier, and trapping and removing pathogens and debris. Currently formulated drugs with micro and nanoparticles were rapidly cleared by ocular mucus.[41] Caffery et.al., revealed that mucin 1 proteins in tear film were increased in patients with Sjogren's DED.[42] Thus, we chose mucin 1 as the delivery target to reduce the clearance by mucus, especially under dry eye conditions. To investigate the effect of the S2.2 aptamer on liposome retention time, we employed a non-aptamer control sequence. Both sequences were conjugated with cholesterol for insertion into liposomes (Scheme 1C). The cholesterol tag enables the aptamer to be inserted on the liposome surface.[30]

After ultracentrifugation, the free aptamers were measured by spectrophotometer. Approximately 83%, 74% and 87% of the initial aptamers were attached to drug-free liposomes (S2.2 aptamer), CsA liposomes (S2.2 aptamer), and CsA liposomes (non-aptamer), respectively. We estimated the number of DNA strands on each liposome to be approximately 673. The calculations are illustrated in **Figure S4.**

Evaluation in a DED cell model

DED is a common ocular disorder that affects millions of people worldwide. It is characterized by a deficiency in the quantity or quality of tears, leading to discomfort, visual disturbance, and potential damage to the ocular surface.[43, 44] The mechanisms underlying the disease are multifactorial, including inflammation, tear film instability, and hyperosmolarity.[45, 46] Under normal conditions, the osmolarity of the tear film is maintained at equilibrium ranging from 296 to 302 mOsM. In patients suffering from DED, however, the osmolarity values are usually elevated and can range from 316 to over 400 mOsmM.[43, 44] Hyperosmolarity, which refers to an increase in the concentration of solutes in the tears, is a common pathway in the development of DED. Most animal and *in vitro* studies of hyperosmolarity in DED have been conducted using elevated osmolarity levels ranging from 400 to 600 mOsM. [43, 44] Specifically, increasing the osmolarity of the medium to over 450 mOsM by adding sodium chloride has been reported

to mimic the situation in DED by inducing cell death and inflammatory cytokine expression (IL-1β, IL-6, IL-8 and TNF-α) in human corneal epithelial cells via the mitogen-activated protein kinase-c-Jun N-terminal kinase and extracellular-regulated kinase pathway.[47-51] These inflammatory markers have also been found in the tears of patients with DED.[52, 53] Therefore, we adopted a dry eye *in vitro* model in HCECs by increasing the osmolarity of the medium to 512 mOsM.

Previous studies have showed that 0.05% CsA could induce cell death in HCECs in 10 min.[54] Thus, we first studied the cytotoxicity of CsA liposomes. As expected, the results in **Figure 2** suggested that increasing the osmolarity of the medium reduced the cell viability of HCECs compared to the control group, while treatment with 0.001% and 0.002% CsA in the medium for 24 h further suppressed the viability of HCECs compared to the DED groups. This implied the cytotoxicity of CsA alone in HCECs. Interestingly, neither the drug-free liposomes nor the CsA liposomes induced cell death in the DED model regardless of dosage, suggesting the encapsulation of CsA in liposomes could lessen the cytotoxic effects of CsA in HCECs.

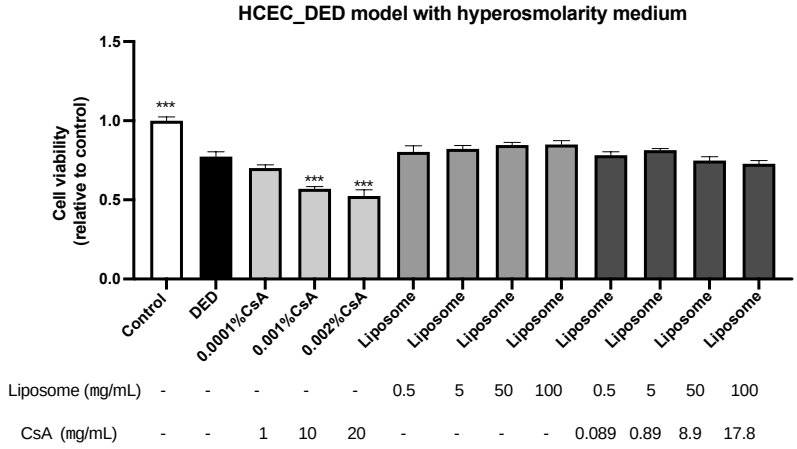

Figure 2 Cytotoxicity of the synthesized liposomes. DED condition in HCECs was induced by hyperosmotic pressure. The cells were treated with free CsA, drug-free liposomes, or CsA liposomes at different concentrations for 24 h. The MTS assay was performed to measure cell viability. Data are shown as mean ± SEM and analyzed using one-way ANOVA analysis. ****P* < 0.001 compared with DED group, n=3.

We then investigated the uptake of liposomes by HCECs. After 4 h, some liposomes were observed to be saturated in the cytoplasm, even after washing out unbound liposomes (**Figure 3A)**. Liposomes coated with a dense layer of DNA are a type of spherical nucleic acids, and they can easily enter cells. One study reported that nanoparticles conjugated with spherical nucleic acids can be internalized by cells via class A scavenger receptors and endocytosed

through a lipid-raft-dependent, caveolae-mediated mechanism.[55] In particular, the fluorescence intensities of liposomes functionalized with S2.2 detected in HCECs were significantly higher than those with non-aptamer controls (**Figure 3C**). There were observable dense clumps of fluorescence signals in the samples incubated with aptamer liposomes, indicating that the S2.2 aptamer could increase the attachment and interaction of liposomes with the cell surface (**Scheme 1D**). To further investigate the retention time of liposomes with S2.2 or non-aptamer coating in HCECs, we prolonged the incubation time to 24 h (20-h incubation in liposome-free medium after washing out unbound liposomes in 4 h). The results in **Figure 3B** showed no observable rhodamine signals in either the control or the non-aptamer CsA liposomes. However, there were remarkable rhodamine signals, albeit weaker than those observed after 4 h, in HCECs treated with both drug-free liposomes and aptamer CsA liposomes, without statistically significant difference between these two groups (**Figure 3C**). These results support the hypothesis that the high affinity and mucin 1-specific aptamer can increase the retention of liposomes in cells.

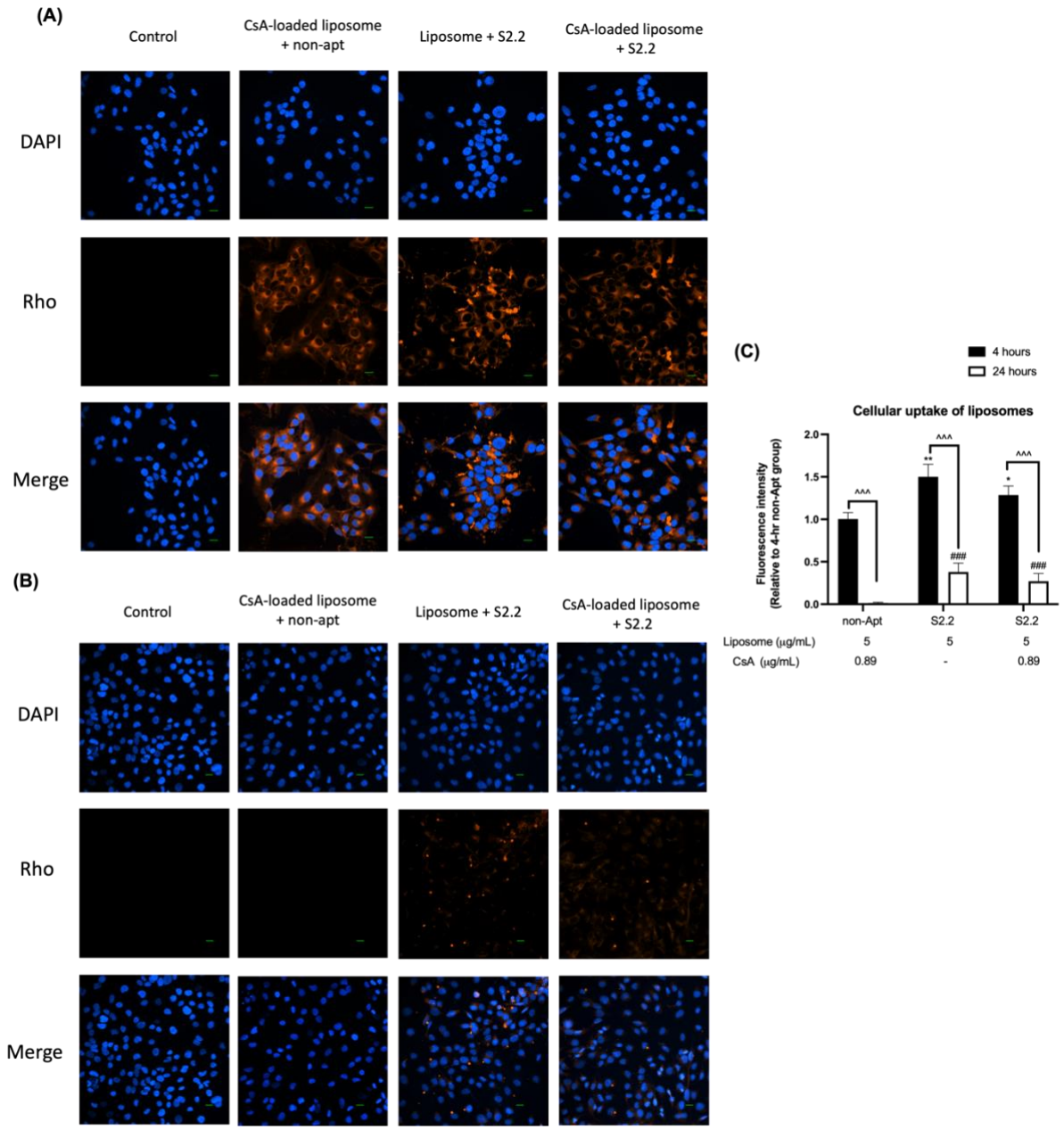

Figure 3 Cellular uptake of the synthesized liposome. (A) Fluorescence images of HCECs incubated with various liposomes for 4 h. (B) Fluorescence images of HCECs incubated with various liposomes for 4 h followed by 20-h incubation in culture medium after washing. The cell nucleus was stained with DAPI to give blue fluorescence and the red fluorescence was from Rhod PE. Scale bars: 20 μm. (C) Quantification of fluorescence intensity. Data are shown as mean ± SEM and analyzed using One-Way ANOVA analysis. $^{*}P < 0.001$, $^{***}P < 0.001$ compared with 4-h non-Apt group; $^{\#\#}P < 0.001$, $^{\#\#\#}P < 0.001$ compared with 24-h non-Apt group; ^^ $P < 0.01$ compared between different time points, n=3. non-Apt: Non-aptamer.

Effect on inflammatory markers

Next, the efficacy of aptamer-functionalized liposome on a dry eye model was investigated. We measured the gene expression levels of three inflammatory markers (IL-6, IL-8, IL-β) in HCECs. These markers were reported to be upregulated in tears in patients with DED and were downregulated by CsA in both *in vivo* and *in vitro* studies.[56] In **Figures 4A-C**, the gene expression levels of three inflammatory markers were increased significantly by hyperosmotic pressure for 24 h compared to control groups. The pre-treatment of CsA dramatically reversed the expression of IL-8, IL-1β at 1 and 10 μg/ml, and IL-6 at 1 μg/ml. Pre-treatment with non-aptamer CsA liposomes or aptamer liposomes at low doses did not exert any anti-inflammatory effect in the DED model of HCECs. Only the treatment of high-dose liposomes containing 0.89 μg/mL suppressed the IL-8, IL-1β genes induced by hyperosmolarity in HCECs. The aptamer CsA liposomes notably reversed the gene expression levels of all inflammatory markers at both doses in DED HCECs. Most importantly, there was no statistical significance between the groups treated with aptamer CsA liposomes and CsA alone, suggesting that their effects were comparable. Furthermore, when comparing the aptamer CsA liposome group to the non-aptamer CsA liposome or aptamer liposome groups, significant alterations in the regulation of IL-6 (**Figures 4A**) and IL-1β (**Figures 4C**) were observed. These changes suggest that the delivery of CsA in liposomes was more effective when used in conjunction with the aptamer.

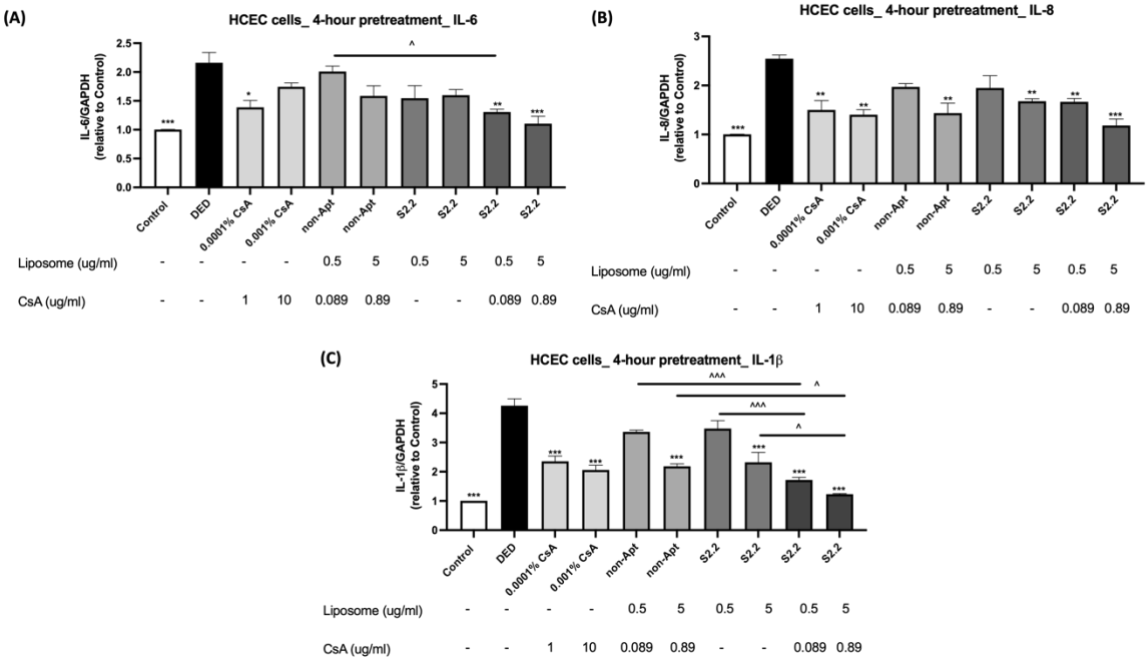

Figure 4 Gene expression levels of dry eye gene markers. The model cells were treated with free CsA, drug-free liposomes, and CsA liposomes at different concentrations for 4 h followed

by 20-h incubation in the culture medium after wash. RT-PCR was performed to measure the mRNA expression levels of (A) IL-6, (B) IL-8 and (C) IL-1β. The data were normalized to GAPDH and relative to the control. Data were shown as mean ± SEM and analyzed using One-Way ANOVA analysis. *$P < 0.05$, **$P < 0.01$, ***$P < 0.001$ compared with DED group, n=3. non-Apt: Non-aptamer.

Corneal epithelial cell permeability assays

Besides inflammation, one of the outcomes of DED is damages to the corneal epithelium, which can result in increased permeability and allow harmful substances to enter the cornea, leading to further damages. [43, 44] Fluorescein uptake and rose bengal staining are commonly used methods to measure the permeability of corneal epithelial cells in animal models. These methods provide quantitative measurements of the extent of epithelial damage and help to evaluate the effectiveness of potential treatments for DED.[57] The results from **Figure 5A** and **Figure S5** showed an increased dye uptake in the DED cell model compared to the control groups (**Figure 5A** and **Figure S5**). All treatments appeared to reduce the uptake of both dyes, indicating that all treatments were effective in regulating cell permeability of HCECs under dry eye conditions. Notably, aptamer CsA liposomes showed significant differences in fluorescence intensity compared to the other two liposome groups (Figure 5B), suggesting that the presence of the S2.2 aptamer and CsA in the liposome provided greater protection against cell permeability in HCECs.

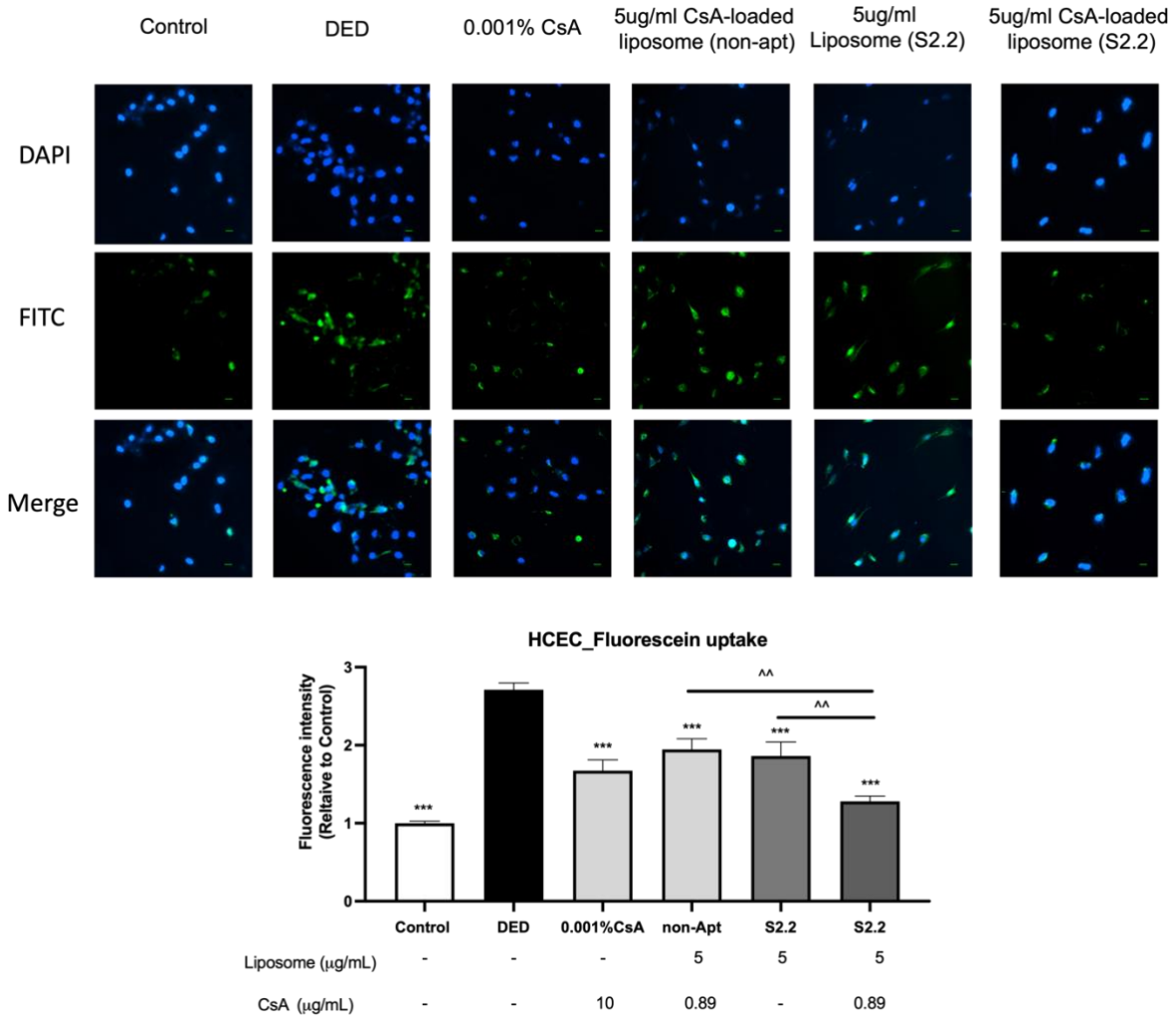

Figure 5 Cell permeability assays. (A) Fluorescence images of treated HCECs incubated with 1 mM fluorescein for 5 min in the culture medium after washing. The cell nucleus was stained with DAPI to give blue fluorescence and the green fluorescence was from fluorescein. Scale bars: 20 μm. (B) Quantification of fluorescence intensity. Data were shown as mean ± SEM and analyzed using One-Way ANOVA analysis. ***$P < 0.001$ compared with DED group; ^^ $P < 0.01$ compared with aptamer CsA liposomes, n=3. non-Apt: Non-aptamer.

The finding that the drug-free liposomes at higher doses worked in inhibiting inflammation and restoring corneal permeability in HCECs was not surprising, as restoring the lipid content in the corneal epithelium to prevent inflammation, evaporation of aqueous in the eye, and subsequent drying is a known therapeutic approach for dry eye disease and corneal injury.[58] This suggests that the presence of liposomes contributed to the anti-inflammatory action of aptamer CsA liposomes *in vitro*. Interestingly, CsA at a lower dose in liposomes (0.089 μg/mL) achieved a comparable effect to CsA alone at higher doses (1 and 10 μg/ml) in HCECs.

Animal model studies

To further evaluate the efficacy of aptamer CsA liposomes in managing DED, an *in vivo* study was performed. Mice, rats, and rabbits are the most commonly used animals for establishing DED models.[59] In animal models, dry eye syndrome is usually induced using benzalkonium chloride (BAC), a common preservative in ophthalmological solutions. BAC may affect ocular surface integrity, and induce tear film instability, epithelial apoptosis, and inflammation.[59, 60] Beyazyıldız et.al., showed the installation of 0.2% BAC for 1 week could induce dry eye syndrome in rats, including reduced tear production and increased inflammation.[61] Thus, the present study established a dry eye disease model on rats induced by BAC installation.

Fluorescein staining of cornea is a reliable clinical way to assess corneal integrity, which is greatly affected by DED.[62] In **Figure 6A**, the DED group showed a large coalescent and patch pattern of fluorescein staining in all five corneal zones (**Figure 6B and Figure S6)**. Treatment with CsA eye drops or aptamer CsA liposomes resulted in a distinct decrease in fluorescein coalescent staining of the cornea in rats. The punctate staining scores were 17.8 ± 0.8, 11 ± 0.5, and 12.5 ± 0.5 in the DED, CsA eye drops, and aptamer CsA liposomes groups, respectively (**Figure S6**). Furthermore, the tear production in rats was measured with threads and indicated as the wet length of the threads. **Figure 6C** showed that the tear production was also enhanced significantly after CsA treatments (5.9 mm) and liposomal treatment (5.2 mm) , compared to the basal level (3.8 mm**)**. These results suggest that aptamer CsA liposomes have a therapeutic effect as CsA eye drops in improving corneal integrity and tear production under dry eye conditions. Previous studies have reported that CsA inhibits a chemokine receptor and regulates inflammatory markers and MMPs expression to produce this effect.[12] When comparing the tear production and fluorescein staining in rats after treatments, there was no statistically significant difference between the two treatment groups, possibly due to the frequency of administration. In addition, the reason for the relatively low tear production, but did not reach statistical significance, in the liposome group could be that CsA in eye drops directly triggered the cellular signaling pathway to increase tear production, while CsA in liposomes might take time to release CsA and take effect. Further studies are needed to evaluate whether the action of S2.2 functionalized CsA liposomes is comparable to frequently administered CsA eye drops, by reducing the frequency of administration, like once a day or thrice a week.

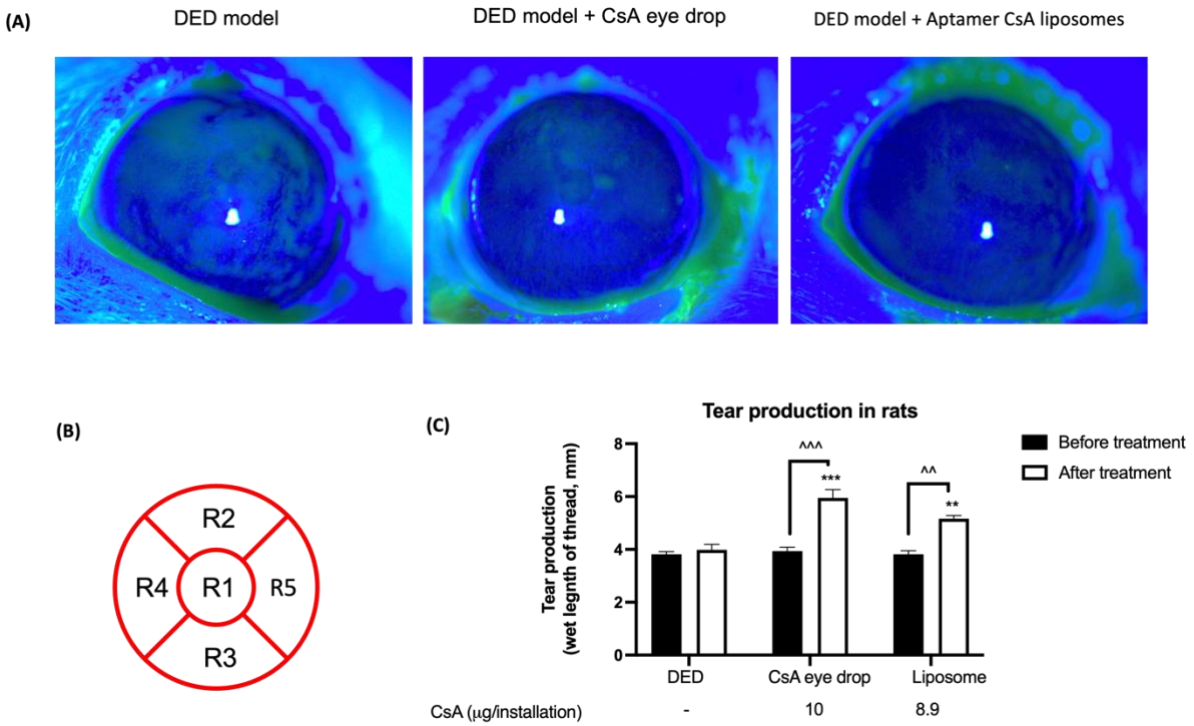

Figure 6 Efficacy of aptamer CsA liposomes in managing DED**.** (A) Representative images of fluorescence staining of the corneal epithelium of rats after 28-day treatment. (B) The cornea was divided into 5 parts for scoring fluorescence punctate staining. (C) Tear production in rats before treatment (basal level in the DED condition) and after 28-day treatment. Data were shown as mean ± SEM and analyzed using One-Way ANOVA analysis. $^{**}P < 0.01$, $^{***}P < 0.001$ compared with DED group; ^^ $P < 0.01$, ^^^ $P < 0.01$ compared with before treatment, n=6.

Conclusions

The particularly promising area in the present study is the use of aptamers, short nucleic acid sequences that can specifically bind to target molecules with high affinity and specificity, for targeted drug delivery to ocular tissues. This is the first study to investigate the use of aptamer-functionalized liposomes for drug delivery to the corneal epithelium. Our data demonstrated that the CsA-loaded liposomes coated with S2.2 had a better retention time and protective effect in HCECs under dry eye conditions, improved tear production, and reduced corneal fluorescein staining in a rat DED model. Future studies should focus on the physiological distribution and efficacy in vivo. It is hoped that the present study will provide a better tool for ocular drug delivery to treat dry eye diseases.

Conflict of interest: The authors declare that they have no conflict of interest.

Acknowledgments: Funding for this work was from the Hong Kong Special Administrative Region Government and InnoHK. We also acknowledge Dr. Maud Gorbet at the University of Waterloo for providing HCECs as gifts.

1. V. Gote, S. Sikder, J. Sicotte and D. Pal, *J. Pharmacol. Exp. Ther.*, 2019, **370**, 602-624.
2. D. D. Nguyen, L. J. Luo, C. J. Yang and J. Y. Lai, *ACS Nano*, 2023, **17**, 168-183.
3. L.-J. Luo, D. D. Nguyen and J.-Y. Lai, *Biomaterials*, 2020, **243**, 119961.
4. J. Willem de Vries, S. Schnichels, J. Hurst, L. Strudel, A. Gruszka, M. Kwak, K.-U. Bartz-Schmidt, M. S. Spitzer and A. Herrmann, *Biomaterials*, 2018, **157**, 98-106.
5. D. D. Nguyen and J.-Y. Lai, *Polym. Chem.*, 2020, **11**, 6988-7008.
6. S. B. K. Dludla, L. T. Mashabela, B. Ng'andwe, P. A. Makoni and B. A. Witika, *Polymers*, 2022, **14**, 3580-3617.
7. F. He, N. Wen, D. Xiao, J. Yan, H. Xiong, S. Cai, Z. Liu and Y. Liu, *Curr. Med. Chem.*, 2020, **27**, 2189-2219.
8. J. Zhou and J. Rossi, *Nat. Rev. Drug Discov.*, 2017, **16**, 181-202.
9. S. A. Vinores, *Int. J. Nanomed.*, 2006, **1**, 263-268.
10. S. A. Moosavian and A. Sahebkar, *Cancer Lett.*, 2019, **448**, 144-154.
11. F. Lallemand, O. Felt-Baeyens, K. Besseghir, F. Behar-Cohen and R. Gurny, *Eur. J. Pharm. Biopharm.*, 2003, **56**, 307-318.
12. L. M. Periman, F. S. Mah and P. M. Karpecki, *Clin. Ophthalmol.*, 2020, **14**, 4187-4200.
13. R. C. de Oliveira and S. E. Wilson, *Clin. Ophthalmol.*, 2019, **13**, 1115-1122.
14. B. Yavuz, S. B. Pehlivan and N. Unlu, *Sci. World J.*, 2012,**2012**, 194848-194858.
15. A. Mandal, V. Gote, D. Pal, A. Ogundele and A. K. Mitra, *Pharm. Res.*, 2019, **36**, 36.
16. D. K. Karumanchi, Y. Skrypai, A. Thomas and E. R. Gaillard, *J. Drug Deliv. Sci. Technol.*, 2018, **47**, 275-282.
17. T. Y. Ren, X. Y. Lin, Q. Y. Zhang, D. M. You, X. Y. Liu, X. G. Tao, J. X. Gou, Y. Zhang, T. Yin, H. B. He and X. Tang, *Mol. Pharm.*, 2018, **15**, 4862-4871.
18. V. Garg, R. Suri, G. K. Jain and K. Kohli, *Colloids Surf. B.*, 2017, **157**, 40-47.
19. H. Qiao, Z. Xu, M. C. Sun, S. W. Fu, F. X. Zhao, D. P. Wang, Z. G. He, Y. L. Zhai and J. Sun, *J. Drug Deliv. Sci. Technol.*, 2022, **75**, 103654-103660.
20. Mohammad, V. Garg, J. Nirmal, M. H. Warsi, D. Pandita, P. Kesharwani and G. K. Jain, *J. Pharm. Sci*., 2022, **111**, 479-484.
21. J. S. Garrigue, M. Amrane, M. O. Faure, J. M. Holopainen and L. Tong, *J. Ocul. Pharmacol. Ther.*, 2017, **33**, 647-661.
22. J. J. Lopez-Cano, M. A. Gonzalez-Cela-Casamayor, V. Andres-Guerrero, R. Herrero-Vanrell and I. T. Molina-Martinez, *Expert Opin. Drug Delivy.*, 2021, **18**, 819-847.
23. S. Y. Liu, C. N. Chang, M. S. Verma, D. Hileeto, A. Muntz, U. Stahl, J. Woods, L. W. Jones and F. X. Gu, *Nano Res.*, 2015, **8**, 621-635.
24. A. Lopez-Machado, N. Diaz-Garrido, A. Cano, M. Espina, J. Badia, L. Baldoma, A. C. Calpena, E. B. Souto, M. L. Garcia and E. Sanchez-Lopez, *Pharmaceutics*, 2021, **13**, 1698-1716.
25. X. Chen, J. C. Wu, X. Q. Lin, X. D. Wu, X. W. Yu, B. Wang and W. Xu, *Front. Pharmacol.*, 2022, **13**, 838168-838183.
26. R. J. Banga, N. Chernyak, S. P. Narayan, S. T. Nguyen and C. A. Mirkin, *J. Am. Chem. Soc.*, 2014, **136**, 9866-9869.

27. Z. H. Cao, R. Tong, A. Mishra, W. C. Xu, G. C. L. Wong, J. J. Cheng and Y. Lu, *Angew. Chem., Int. Ed.*, 2009, **48**, 6494-6498.
28. M. J. Lin, Y. Y. Chen, S. S. Zhao, R. Tang, Z. Nie and H. Xing, *Angew. Chem., Int. Ed.*, 2022, **61**.
29. Y. Liu, K. M. Castro Bravo and J. Liu, *Nanoscale Horiz.*, 2021, **6**, 78-94.
30. A. Lopez and J. Liu, *Langmuir*, 2018, **34**, 15000-15013.
31. A. A. Ali, Y. Bagheri and M. X. You, *Q. Rev. Biophys.* 2022, **55**, 1-11.
32. S. Molladavoodi, M. Robichaud, D. Wulff and M. Gorbet, *PLoS One*, 2017, **12**, e0178981-e0178996.
33. K. Sall, G. N. Foulks, A. D. Pucker, K. L. Ice, R. C. Zink and G. Magrath, *Clin. Ophthalmol.*, 2023, **17**, 757-767.
34. P. Liu, G. Chen and J. Zhang, *Molecules*, 2022, **27**, 1372-1394.
35. S. M. Shaheen, F. Shakil Ahmed, M. N. Hossen, M. Ahmed, M. S. Amran and M. Ul-Islam, *Pak. J. Biol. Sci.*, 2006, **9**, 1181-1191.
36. A. Akbarzadeh, R. Rezaei-Sadabady, S. Davaran, S. W. Joo, N. Zarghami, Y. Hanifehpour, M. Samiei, M. Kouhi and K. Nejati-Koshki, *Nanoscale Res. Lett.*, 2013, **8**, 102-102.
37. M. Guimarães Sá Correia, M. L. Briuglia, F. Niosi and D. A. Lamprou, *Int. J. Pharm.*, 2017, **516**, 91-99.
38. D. Patel, S. Patel and D. Pathak, *Int. J. Pharm. Qual. Assur*., 2020,**11**,196-204.
39. P. R. Cullis, L. D. Mayer, M. B. Bally, T. D. Madden and M. J. Hope, *Adv. Drug Deliv. Rev.*, 1989, **3**, 267-282.
40. C. S. Ferreira, C. S. Matthews and S. Missailidis, *Tumour Biol*, 2006, **27**, 289-301.
41. A. Popov, *J. Ocul. Pharmacol. Ther.*, 2020, **36**, 366-375.
42. B. Caffery, M. L. Heynen, E. Joyce, L. Jones, R. Ritter, 3rd and M. Senchyna, *Mol. Vis.*, 2010, **16**, 1720-1727.
43. A. Alejandro and B. Alejandro, in *Ocular Surface Diseases*, ed. K. Dorota, IntechOpen, Rijeka, 2020, DOI: 10.5772/intechopen.90113, Ch. 3.
44. C. Baudouin, P. Aragona, E. M. Messmer, A. Tomlinson, M. Calonge, K. G. Boboridis, Y. A. Akova, G. Geerling, M. Labetoulle and M. Rolando, *Ocul. Surf.*, 2013, **11**, 246-258.
45. S. C. Pflugfelder and C. S. de Paiva, *Ophthalmology*, 2017, **124**, S4-S13.
46. J. P. Craig, K. K. Nichols, E. K. Akpek, B. Caffery, H. S. Dua, C. K. Joo, Z. Liu, J. D. Nelson, J. J. Nichols, K. Tsubota and F. Stapleton, *Ocul. Surf.*, 2017, **15**, 276-283.
47. M. Zhao, L. Liu, Y. Zheng, G. Liu, B. Che, P. Li, H. Chen, C. Dong, L. Lin and Z. Du, *RSC Adv.*, 2019, **9**, 12998-13006.
48. X. Hua, R. Deng, J. Li, W. Chi, Z. Su, J. Lin, S. C. Pflugfelder and D. Q. Li, *Invest. Ophthalmol. Vis. Sci.*, 2015, **56**, 5503-5511.
49. Y. Ren, H. Lu, P. S. Reinach, Q. Zheng, J. Li, Q. Tan, H. Zhu and W. Chen, *Sci. Rep.*, 2017, **7**, 4727-4737.
50. Z. Liu, D. Chen, X. Chen, F. Bian, N. Gao, J. Li, S. C. Pflugfelder and D.-Q. Li, *Int. J. Mol. Sci.* 2020, **21**, 8966-78.
51. T. Panigrahi, S. D'Souza, R. Shetty, A. Padmanabhan Nair, A. Ghosh, E. Jacob Remington Nelson, A. Ghosh and S. Sethu, *Clin. Transl. Sci.*, 2021, **14**, 288-298.
52. N. Boehm, A. I. Riechardt, M. Wiegand, N. Pfeiffer and F. H. Grus, *Invest. Ophthalmol. Vis. Sci.*, 2011, **52**, 7725-7730.
53. M. Tamhane, S. Cabrera-Ghayouri, G. Abelian and V. Viswanath, *Pharm. Res.*, 2019, **36**.
54. J. E. Lee, W. B. Shin and J. S. Lee, *J. Korean Ophthalmol. Soc.*, 2007, **48**, 1399-1409.

55. C. H. Choi, L. Hao, S. P. Narayan, E. Auyeung and C. A. Mirkin, *Proc. Natl. Acad. Sci. U. S. A.*, 2013, **110**, 7625-7630.
56. H. J. YOON, Y. Li, R. J. Jin, J.-H. Choi, J. H. Yu and K. C. Yoon, *Invest. Ophthalmol. Vis. Sci.*, 2018, **59**, 3836-3836.
57. H. M. Tabery, *Eye (Lond)*, 2003, **17**, 482-487.
58. J. S. Fogt, M. J. Kowalski, P. E. King-Smith, A. T. Epitropolous, A. J. Hendershot, C. Lembach, J. P. Maszczak, L. A. Jones-Jordan and J. T. Barr, *Clin. Ophthalmol.*, 2016, **10**, 2237-2243.
59. M. M. Rahman, D. H. Kim, C. K. Park and Y. H. Kim, *Int. J. Mol. Sci.*, 2021, **22**, 12102-12129.
60. C. Baudouin, A. Labbé, H. Liang, A. Pauly and F. Brignole-Baudouin, *Prog. Retin. Eye Res.*, 2010, **29**, 312-334.
61. E. Beyazyildiz, E. R. Hekimoglu, G. Sobaci, O. Beyazyildiz, A. Albayrak, F. A. Pinarli, M. N. Demir, T. Delibasi, F. Kaymaz and U. Acar, *Stem cells int.*, 2014, **2014**, 250230-250239.
62. M. Mokhtarzadeh, R. Casey and B. J. Glasgow, *Invest. Ophthalmol. Vis. Sci.*, 2011, **52**, 2127-2135.

Electronic supplementary information

Mucin-targeting-aptamer functionalized liposomes for delivery of cyclosporin A for dry eye diseases

Ka-Ying Wong[1,2], Yibo Liu[1,2], Liping Zhou[1,3,4,5], Man-Sau Wong[1,3,4], Juewen Liu*[1,2]

[1]Centre for Eye and Vision Research (CEVR), 17W Hong Kong Science Park, Hong Kong;
[2]Department of Chemistry, Waterloo Institute for Nanotechnology, University of Waterloo, Waterloo, ON, N2L 3G1, Canada

[3]Department of Food Science and Nutrition, The Hong Kong Polytechnic University, Hung Hom, Kowloon, Hong Kong SAR, PR China

[4]Research Center for Chinese Medicine Innovation, The Hong Kong Polytechnic University, Hung Hom, Kowloon, Hong Kong SAR, PR China

[5] School of Optometry, The Hong Kong Polytechnic University, Hung Hom, Kowloon, Hong Kong SAR, PR China

Authors' email addresses:
Ka-Ying Wong: **kaya.wong@cevr.hk**
Yibo Liu: **xiaonao0526@hotmail.com**
Liping Zhou: **lp.zhou@polyu.edu.hk**
Man-Sau Wong: **man-sau.wong@polyu.edu.hk**
Juewen Liu: liujw@ uwaterloo.ca

Corresponding author: Prof. Juewen Liu (liujw@ uwaterloo.ca)

Table S1. Primer sequences for real-time PCR to quantify mRNA expression of various genes.

Gene	Primer	Primer sequence (5'->3')
IL-1β	Forward	CCTGTCCTGCGTGTTGAAAGA
	Reverse	GGGAACTGGGCAGACTCAAA
IL-6	Forward	CACAGACAGCCACTCACCTC
	Reverse	TTTTCTGCCAGTGCCTCTTT
IL-8	Forward	TTTCAGAGACAGCAGAGCACACAA
	Reverse	CACACAGAGCTGCAGAAATCAGG
GAPDH	Forward	GAAGGTGAAGGTCGGAGTC
	Reverse	GAAGATGGTGATGGGATTTC

Table S2. Quantification of CsA in combined liposomes.

	10 wt.%	20 wt.%	40 wt.%	50 wt.%
Total CsA				
Absorbance at 205 nm [CsA loaded liposome – liposome]	**0.2**	**0.3**	**0.2**	**0.3**
Total CsA (µg/ml) in liposome (5mg/ml)	**502.7**	**895.4**	**605.0**	**772.2**
Unloaded CsA				
Absorbance at 205 nm [CsA loaded liposome – liposome]	**0.01**	**0.03**	**0.06**	**0.08**
Unloaded CsA (µg/ml) in liposome (5mg/ml)	**10.1**	**17.1**	**23.8**	**29.9**
Drug loading content (%)				
(Weight of CsA in Liposome / Weight of liposome) x 100	**9.9**	**17.6**	**11.6**	**14.8**
Encapsulation efficiency (%)				
((Weight of total CsA – weight of unloaded CsA)/ Weight of initial CsA) x 100	**97.5**	**87.8**	**29.1**	**26.7**

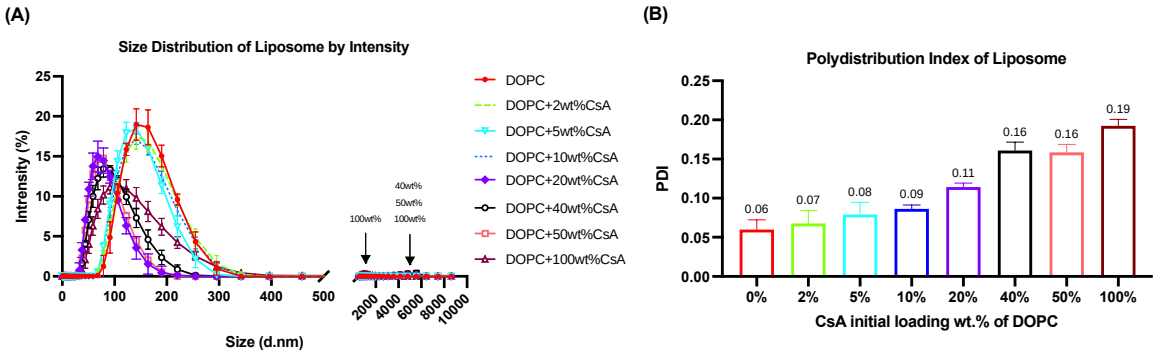

Figure S1. Size analysis of liposome by DLS. (A) The size distribution of liposomes and (B) PDI with different CsA loading by intensity. n=3. The measurements were performed in PBS at 25 ºC.

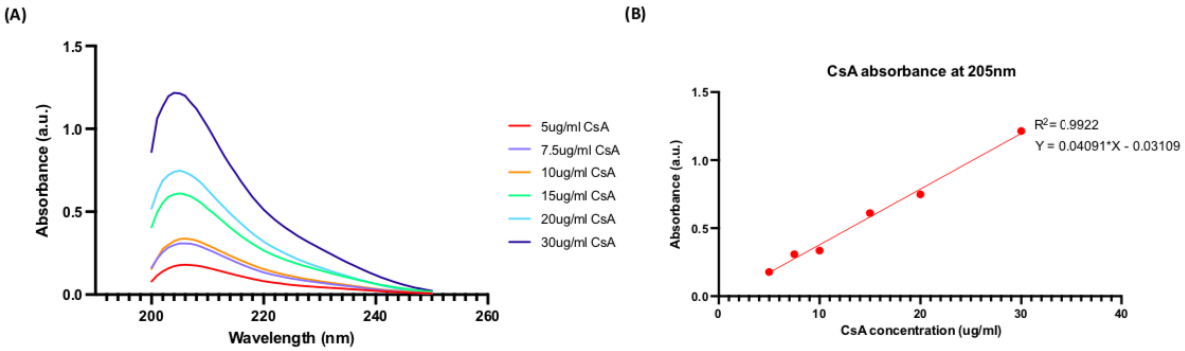

Figure S2. Construction of standard curve for CsA quantification using UV-vis spectrometry in 90% ethanol. (A) UV spectra of various concentrations of CsA. (B) Calibration curve of CsA at various concentrations based on the absorbance at 205 nm. n=1.

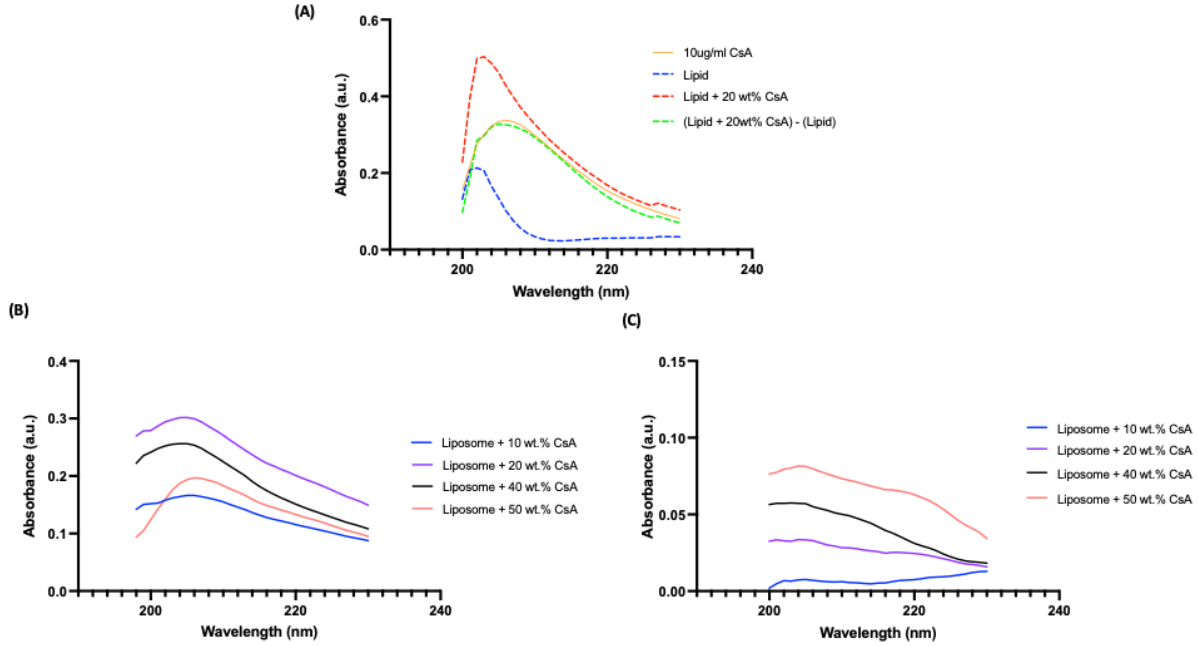

Figure S3. UV spectrum of total CsA and free CsA in samples. (A) UV absorbance of free CsA, lipid molecules, and drug loaded CsA. (B) UV absorbance of total CsA in samples after normalization with lipid molecules. (C) UV absorbance of unloaded CsA in samples after normalization with lipid molecules. n=1.

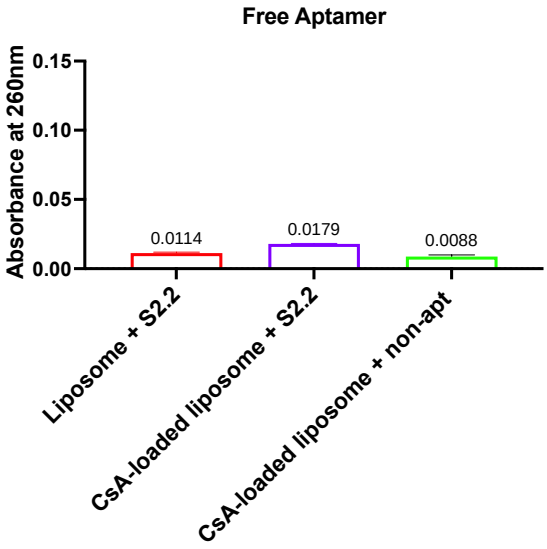

Figure S4. Free aptamer analysis by spectrophotometer at 260 nm and calculations of DNA loading density on liposomes. n=3.

The free aptamer was separated from the liposome by ultracentrifugation at 120,000 rpm for 30 min, and the concentrations of free aptamer were determined using a spectrophotometer at 260 nm. The absorbances of the free aptamer in the aptamer liposome, aptamer CsA liposome, and non-aptamer CsA liposome groups were 0.0114, 0.0179, and 0.0088, respectively. Using the Beer-Lambert Law (path length of 0.05 cm) and the extinction coefficients of S2.2 and non-aptamers (200201 and 272201, respectively), the amounts of free aptamers in a 200 μL reaction were calculated as 166.9 pmol, 262.1 pmol, and 128.8 pmol in the aptamer liposomes, aptamer CsA liposomes, and non-aptamer CsA liposomes, respectively. By subtracting the amount of free aptamers from the initial amount of aptamers (1000 pmol), the approximate amounts of conjugated aptamers were 833 pmol (83% of the initial amount of aptamer), 738 pmol (74%), and 871 pmol (87%) in these groups, respectively.

To estimate the DNA density on liposomes, we calculated that 20 μL of 5.0 mg/mL liposome can adsorb an average of 814 pmol DNA. The molar concentration of phospholipid (5.0 mg/mL) was 6.34 mM, with a total mole of phospholipids at 6.34 μmol. Based on the DLS results, the average particle size of the 20% CsA loading group was 106 nm. Using these values, we estimated that each liposome contains approximately 105,000 phospholipid molecules, assuming the phospholipid head group was 0.6 nm. The effect of cholesterol on expanding or shrinking the average size of the phospholipid head groups was not considered in this estimation. Therefore, the amount of liposome was calculated as 6.34 mM × 20 μL / 105,000 = 1.21 pmol, and each 106 nm liposome contained 673 DNA molecules on average.

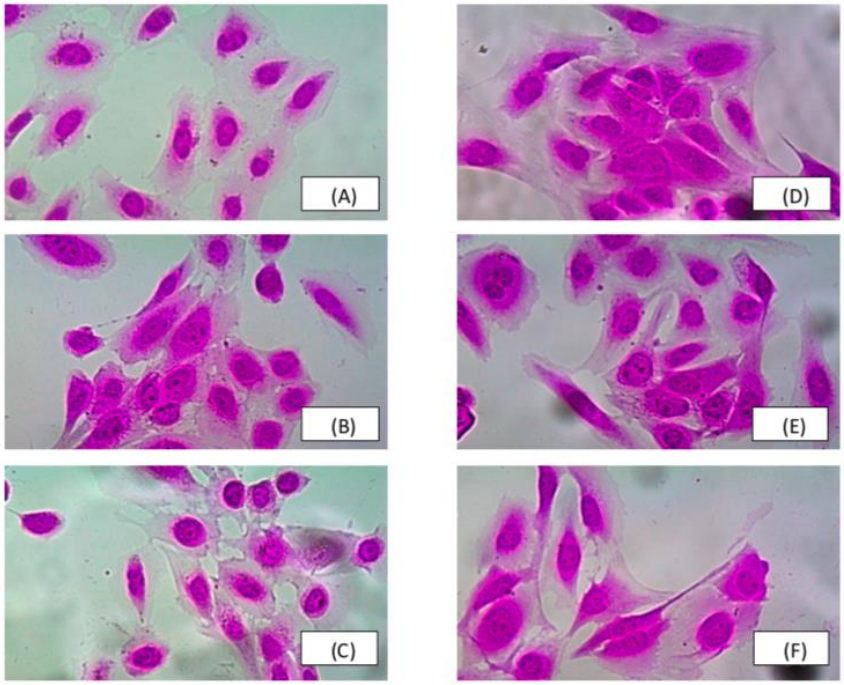

Figure S5. Rose bengal uptake in treated HCECs. (A) Control, (B) DED, (C) 0.001% CsA , (D) 5 μg/mL non-aptamer CsA liposomes, (E) 5 μg/mL aptamer liposomes and (F) 5 μg/mL aptamer CsA liposomes. n=3.

(A)

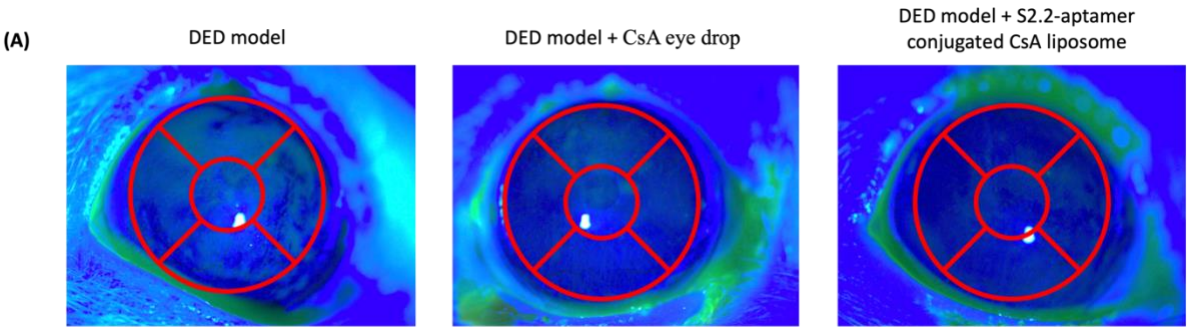

(B)

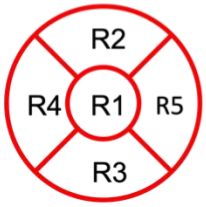

(C)

	Estimated mean fluorescein punctate staining score (sum of five regions)
DED model	17.8 ± 0.8
DED model + 0.1%CsA eye drop	11 ± 0.5**
DED model + S2.2-aptamer conjugated CsA liposome	12.5 ± 0.5 **

Figure S6. Evaluation of fluorescein punctate staining score on rat cornea. n=6. Data are shown as mean ± SEM and analyzed using One-Way ANOVA analysis. $^{**}P < 0.01$ compared with DED group.